



# Extinction, Turnover, and the Reorganization of Diatom Communities Across the Eocene/Oligocene Boundary: Equatorial Atlantic Perspective

Volkan Özen<sup>1</sup>, Johan Renaudie<sup>2</sup>, David Lazarus<sup>2</sup>

5 <sup>1</sup>Freie Universität Berlin, Institute for Geological Sciences, Malteserstraße 74–100, 12249 Berlin, Germany

<sup>2</sup>Museum für Naturkunde, Leibniz Institute for Evolution and Biodiversity Science, Invalidenstraße 43, 10115 Berlin, Germany

*Correspondence to:* Volkan Özen (volkan.oezen@fu-berlin.de)

**Abstract.** Marine diatoms couple the global carbon and silicon cycles, and their fossil record tracks oceanographic and climatic changes in deep-time. The Eocene/Oligocene Transition (EOT) marks the onset of Antarctic glaciation and major ocean reorganization and is a key interval in diatom evolutionary history. Although high-latitude plankton responses to polar cooling are extensively studied, it remains challenging to determine how cooling-driven changes in circulation, stratification and nutrient supply propagated and shaped low-latitude assemblages. Here we reconstruct species-level diatom diversity from exhaustive full-assemblage counts and integrate these data with diatom and radiolarian productivity from Deep Sea Drilling Project (DSDP) Site 366 (Sierra Leone Rise, equatorial Atlantic) spanning 38–32 Ma. Diatom diversity at DSDP 15 366 varies in step with Southern Ocean diversity records across the same interval. Extinction rates and community-structure metrics indicate a major reorganization of tropical diatom communities that is consistent with changes in upper-ocean stratification. We identify a sharp shift in community structure at ~33.5 Ma, pointing to a rapid ecological response in the earliest Oligocene.

## 20 **1 Introduction**

The relationship between plankton and climate is central to understanding ocean ecosystems and global biogeochemical cycles. Through photosynthesis and particle export, phytoplankton regulate carbon exchange between the atmosphere and the ocean interior, shaping both marine productivity and climate feedback (e.g., Eppley and Peterson, 1979; Kwon et al., 2009; De La Rocha and Passow, 2014; Nowicki et al., 2022; Siegel et al., 2023). Among phytoplankton, diatoms hold a 25 unique position by welding together the global carbon and silicon cycles through their minute siliceous shells. Although they contribute less than one quarter of total marine primary productivity, they account for roughly 40% of the organic carbon exported from surface waters to the deep ocean (Jin et al., 2006; Tréguer et al., 2018; Behrenfeld et al., 2021). By mediating these key fluxes, diatoms influence ocean chemistry and climate from seasonal to geological timescales (e.g., Yool and Tyrrell, 2003; Ragueneau et al., 2006; Renaudie, 2016; Tréguer et al., 2021). Yet their long-term ecological responses to



30 climate change remain far from being resolved, because most reconstructions of diversity dynamics rely on biostratigraphic  
data compilations rather than quantitative, species-level assessments (e.g., Rabosky and Sorhannus, 2009; Lazarus et al.,  
2014; Crampton et al., 2016). While these compilations have provided a valuable framework for interpreting large-scale  
evolutionary trends, they offer only a coarse view of past macroevolutionary behavior (Lazarus, 2011). Developing species-  
level, quantitative reconstructions of diatom communities are therefore essential to understand how marine ecosystems  
35 responded to major climatic transitions.

Among major Cenozoic climatic transitions, the late Eocene to early Oligocene transition (hereafter EOT, in this work we  
focus on a 38 to 32 Ma range) stands out as a pivotal interval for investigating how diatom communities responded to large-  
scale cooling and oceanographic reorganization. Progressive Paleogene cooling culminated at this time in the establishment  
40 of a permanent Antarctic ice sheet and a major reorganization of ocean circulation (e.g., Kennett, 1977; Barker, 2001;  
Zachos et al., 2001; Westerhold et al., 2020; Lear et al., 2008; Coxall et al., 2005; Hutchinson et al., 2021; Galeotti et al.,  
2022). Diatom assemblages experienced major ecological and taxonomic restructuring, accompanied by a marked rise in  
biogenic productivity and opal accumulation (Fenner, 1982, 1985, 1986; Baldauf and Barron, 1990; Lazarus et al., 2014;  
Renaudie, 2016; Rodrigues de Faria et al., 2024; Özen et al., 2025b). These shifts signal a large-scale reorganization of  
45 ocean circulation during the EOT, consistent with the established coupling between biogenic opal deposition and  
oceanographic dynamics (Lisitzin, 1972; Miskell et al., 1985; Baldauf and Barron, 1990; Cortese et al., 2004). Nevertheless,  
identifying the processes that control opal deposition remains challenging, because variations in productivity, circulation,  
and preservation interact differently across ocean basins and through time, obscuring the primary drivers (Ragueneau et al.,  
2000, 2006; Cortese et al., 2004; Renaudie, 2016; Westacott et al., 2021).

50 Regional records illustrate this complexity. In the Southern Ocean, biosiliceous productivity rose sharply in the Late Eocene,  
likely linked to the deepening of Southern Ocean gateways and the nascent Antarctic Circumpolar Current (Diekmann et al.,  
2004; Schumacher and Lazarus, 2004; Anderson and Delaney, 2005; Renaudie, 2016; Rodrigues de Faria et al., 2024; Özen  
et al., 2025b). In the North Atlantic, enhanced biosiliceous accumulation in neritic settings, where diatoms dominated the  
55 plankton assemblages during the Late Eocene (Witkowski et al., 2020), while records show elevated diatom deposition at  
equatorial Atlantic topographic highs such as Deep Sea Drilling Project (DSDP) Site 366 (east equatorial Atlantic; Fig. 1)  
and Ocean Drilling Program (ODP) Site 925 (west equatorial Atlantic; Fig. 1) (Fenner, 1982; Barron and Baldauf, 1989;  
Baldauf and Barron, 1990; Nilsen et al., 2003). In contrast, radiolarians dominated Eocene biosiliceous deposition in the  
equatorial Pacific, with diatoms expanding only in the Early Oligocene when large centric taxa proliferated (~33–32 Ma) in  
60 response to thermocline shoaling and enhanced nutrient supply (Moore et al., 2014). Collectively, these patterns reveal that  
biosiliceous deposition across the EOT was asynchronous and regionally variable, reflecting spatially heterogeneous and  
temporally offset responses in global silica cycling and surface productivity. As polar cooling intensified, diatom  
assemblages became increasingly provincial (Fenner, 1985), yet this provincialism did not translate into true endemism



(Baldauf and Barron, 1990; Baldauf and Manjoniel, 1989). The occurrence of several Early Oligocene species in both  
65 hemispheres' polar regions instead indicates that cross-equatorial dispersal pathways persisted despite strengthened thermal  
gradients (Barron and Baldauf, 1989; Baldauf and Barron, 1990; Gladenkov, 2016).

Within this broader framework, the equatorial Atlantic represents a key region of interhemispheric oceanographic and  
climatic interactions (e.g., Brandt et al., 2023). During the Late Eocene, its eastern sector served as a critical gateway for  
70 deep-ocean circulation (Jones et al., 1995; Wagner, 2002). Although the timing remains poorly constrained,  
sedimentological evidence, including erosional structures, suggests increasing deep-water activity in this region (Stein and  
Faugères, 1989; Jones et al., 1995), pointing to the emergence of an abyssal circulation system resembling the modern  
Atlantic Meridional Overturning Circulation (AMOC). Indeed, the onset of AMOC in the late Eocene has been proposed as a  
mechanism that may have contributed to changing global heat distribution and Antarctic glaciation (Borrelli et al., 2014;  
75 Elsworth et al., 2017). Biogenic opal records from in eastern and western equatorial Atlantic (DSDP Site 366 and ODP Site  
925; Fig. 1) document a pronounced rise in accumulation and shifts in diatom assemblages beginning in the Middle- to Late-  
Eocene transition (~38–36 Ma; Fenner, 1982; Nilsen et al., 2003) and continuing through the EOT, paralleling widespread  
ecological and productivity shifts: taxonomic reorganizations among diatoms and radiolarians in southern high latitudes  
(Funakawa and Nishi, 2008; Pascher et al., 2015; Özen et al., 2025a), evolutionary responses in coccolithophores at southern  
80 mid-latitudes (Ma et al., 2023), increased productivity and opal flux in the southern high-latitudes (Diester-Haass and Zahn,  
1996; Diekmann et al., 2004; Anderson and Delaney, 2005; Pascher et al., 2015; Rodrigues de Faria et al., 2024; Özen et al.,  
2025b), and enhanced opal accumulation in the northern mid-latitudes (Witkowski et al., 2021). This temporal coherence  
across the EOT points to coordinated ecosystem responses to global climate perturbations. Understanding how these  
perturbations propagated throughout the Atlantic basin to reshape diatom diversity, productivity and community structure is  
85 essential for identifying the mechanisms that drove diatom biogeographic and ecological reorganization during this  
transition.

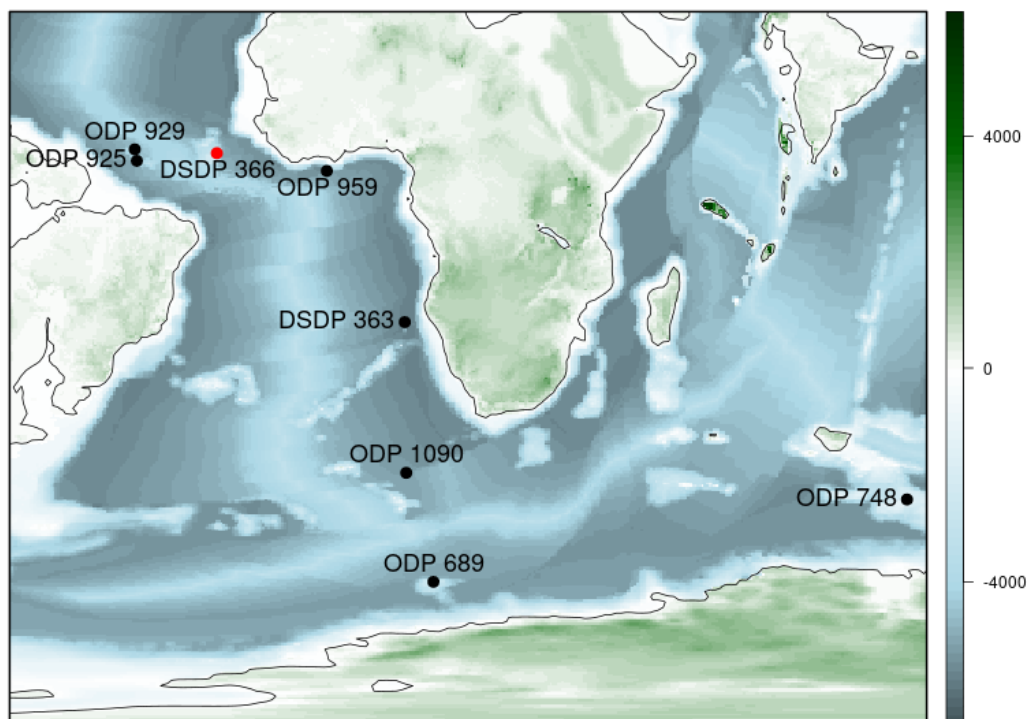
While these regional patterns outline the large-scale reorganization of marine ecosystems, resolving how diatom  
communities responded at the species level remains a key challenge. Quantitative, species-level reconstructions of diatom  
90 diversity across the EOT (or the Cenozoic) remain scarce, particularly from low-latitude settings. Earlier work by Fenner  
(1982; 1984) laid the foundation for understanding diatom diversity in the eastern equatorial Atlantic across this interval (see  
also Corliss et al., 1984). Recent advances from Southern Ocean studies now provide an updated view of high-latitude  
diatom community dynamics (Özen et al., 2025a; 2025b), revealing complex ecological responses to cooling and glaciation.  
Understanding how tropical diatom assemblages responded to these high-latitude climatic changes is critical for assessing  
95 the role of low-latitude regions in global biogeochemical cycling and climate feedback. The equatorial Atlantic is  
particularly well suited to address this question through the diatom record: as a region of interhemispheric oceanographic  
exchange, it likely preserves both direct and indirect responses to circulation changes and Antarctic climate forcing.



Here, we present for the first time a quantitative, full-assemblage based reconstruction of diatom species diversity in the eastern equatorial Atlantic spanning approximately 38 to 32 Ma, based on DSDP Site 366 (Sierra Leone Rise, NW Africa; Fig. 1). This dataset enables us to address the following key questions: (1) How did diatom diversity dynamics and community composition evolve in the equatorial Atlantic across the EOT? (2) Did changes in the equatorial Atlantic diatom assemblages align temporally with climatic and oceanographic shifts documented in the southern high latitudes? (3) What do shifts in the relative productivity of diatoms versus radiolarians reveal about nutrient dynamics and water column structure during this interval? By integrating diversity patterns with accumulation rates and community composition analysis, we aim to provide new insights into the coupling between low-latitude marine ecosystems and global climate change during the EOT.

## 2 Methods

We analyzed 14 samples collected between 396 and 499 meters below sea floor (mbsf), spanning Core 8, Section 2 to Core 19, Section 1 of DSDP Site 366 (Sierra Leone Rise; Fig. 1; Lancelot et al., 1978) in the eastern equatorial Atlantic encompassing the EOT. Of these, 12 samples were used to collect diatom diversity data, samples from Cores 17 and 19 were virtually barren of diatoms and radiolarians. However, these samples were considered in the interpretation of opal abundance, as the absence of biogenic silica provides hints into the diagenetic alteration of the biogenic siliceous record which is a critical mechanism that should be incorporated into diatom studies.



115

**Figure 1: Paleogeographic reconstruction of the late Eocene (35 Ma) showing the location of DSDP Site 366 (red). Additional sites on the map were referenced in discussions synthesizing DSDP 366 results within regional and global frameworks. Paleogeography and paleobathymetry adapted from Straume et al. (2024).**

The biogenic opal record of the equatorial Atlantic is limited to a few sites (Barron et al., 2015), with DSDP Site 366 standing out as one of the key records. This site preserves a continuous (~90 m) sequence of biogenic opal spanning the EOT. Diatom preservation within this interval has been qualitatively described as ‘good’ (Fenner, 1982, 1986; Corliss et al., 1984). The most detailed study of this section to date was carried out by Fenner (1982), who reported continuous diatom occurrence from Core 16 to Core 6. Our observations confirm that dissolution did not significantly affect the Late Eocene and Early Oligocene intervals. However, diatom (and radiolarian) abundance and preservation are closely coupled, as export flux must exceed a threshold in the surface ocean to overcome dissolution and allow effective sequestration (e.g., Takahashi, 1991; Kiørboe, 1993; Jackson, 2001).

## 2.1 Sample preparation

Microscope slides were prepared following the procedures of Moore (1973) and Lazarus (1994), with a modification involving the use of a 10  $\mu\text{m}$  sieve for diatoms. Approximately 0.5 gram of dry sediment was treated sequentially with hydrogen peroxide ( $\text{H}_2\text{O}_2$ ) and pentasodium triphosphate ( $\text{Na}_5\text{P}_3\text{O}_{10}$ ) under low heat, followed by hydrochloric acid (HCl),

130



before sieving. A measured portion of the residue was then allowed to settle randomly onto three coverslips placed at the bottom of a beaker, following the method described by Lazarus (1994).

## 2.2 Diatom and radiolarian mass accumulation rates

To determine the absolute abundances ( $ab$ ) of diatoms and radiolarians, specimens were enumerated within a specific area on the slides. These values were calculated using the following equation:

$$ab = N \times \left(\frac{A_b}{A_m}\right) \times \left(\frac{V_p}{V_u}\right) \times \left(\frac{1}{w}\right)$$

In this equation,  $N$  represents the number of specimens counted, while  $A_b$  and  $A_m$  denote the beaker area (6079 mm<sup>2</sup>) and the measured area (in mm<sup>2</sup>), respectively.  $V_p$  refers to the total volume of prepared residue (mL),  $V_u$  is the volume actually used (mL) and  $w$  is the dry sediment weight (g).

We subsequently derived accumulation rates by calculating the product of the absolute abundance, the dry bulk density based on shipboard measurements, and the linear sedimentation rates (LSR). The LSRs were determined using the revised age model for DSDP Site 366 which can be found in Supplementary Text S1.

## 2.3 Diatom diversity and its dynamics

In this study diversity is defined as total species richness. A total of 14,446 diatom specimens from 12 samples were counted (Supplementary Diversity Data). The counting procedure followed Renaudie and Lazarus (2013), with species-level identifications made whenever possible. Counting continued until at least 1,000 specimens were recorded, though this threshold varied depending on diatom abundance. In samples with low diatom abundance, all observable specimens were counted to maximize taxonomic resolution.

Species identifications were based primarily on published descriptions, especially Fenner's (1982, 1984) work on the equatorial Atlantic. When existing species concepts proved insufficient, or when consistent morphological features did not match documented taxa, specimens were assigned to provisional categories. Each category was documented with reference images and concise, keyword-based differential diagnoses to ensure clarity and reproducibility. We note that all identifications were made using light microscopy, and some species concepts may be revised with future SEM-based work. A complete catalog of all taxa observed in this study is archived on Zenodo, <https://doi.org/10.5281/zenodo.18723713> (Özen et al., 2026).



Raw species counts underestimate true diversity because of variable sampling effort, incomplete detection of rare species, preservation differences, and taxonomic uncertainties. We applied the Chao1 estimator (Chao, 1984) to correct diversity values for unseen taxa and calculated 95 percent confidence intervals for each estimate. This approach provides a more accurate measure of diatom diversity by compensating for differences in sample coverage and allows for more consistent comparison across samples.

#### 2.4 Extinction rates

Determining true extinction horizons is challenging because stratigraphic records are incomplete and species occurrences are sparse. As a result, observed species ranges typically underestimate their actual temporal ranges. Although no method can fully resolve this discrepancy, accounting for temporal gaps in species occurrences allows more realistic estimates of taxon longevity (Marshall, 1997). To do this, we applied a range-estimation approach in which the 50th percentile of observed occurrence gaps was added to each species' first and last appearance datums (FADs and LADs), refining estimates of their temporal ranges.

Extinction rates (lineages per million years) were then calculated using Foote's boundary-crosser method (Foote, 2000). Species occurrences were adjusted using their refined FADs and LADs: if an estimated range extended across a sampled horizon, the species was treated as present in that sample. This procedure incorporates improved range estimate while retaining sample-level resolution and avoids the loss of precision that would result from time-binning.

#### 2.5 Community similarity

To understand assemblage evolution across the EOT, we calculated sample-to-sample community similarity using the Bray-Curtis similarity index (Bray and Curtis, 1957), which ranges from 0 (no similarity) to 1 (complete similarity). This measure is commonly used in ecological studies (Magurran, 2004, p. 174; Clarke and Warwick, 2001) and is useful to apply here because the total number of specimens counted in each sample is similar, so sampling is not severely uneven.

Beyond community similarity, we examined rank-abundance shifts of the most common species in the Eocene and Oligocene to assess assemblage reorganization across the Eocene/Oligocene boundary (E/O). We also calculated pairwise Spearman rank correlations (Spearman, 1904) of log-abundance values between samples. To evaluate shifts in these correlations across the boundary, we compared the distributions of within-epoch correlations (Eocene-Eocene and Oligocene-Oligocene) with cross- Eocene/Oligocene boundary (Eocene-Oligocene) correlations using the Mann-Whitney U test (Mann and Whitney, 1947). This approach allowed us to quantify diatom assemblage change across the Eocene/Oligocene boundary while distinguishing shifts that are independent of extinction patterns.



Using our species-level diversity dataset (see Supplementary Diversity Data), we further investigated environmental signals reflected by changing dominant diatom genera. We first excluded rare genera by retaining only genera with a peak relative abundance of 10% or greater, and subsequently re-normalized remaining genera to give their normalized relative abundance for each studied sample.

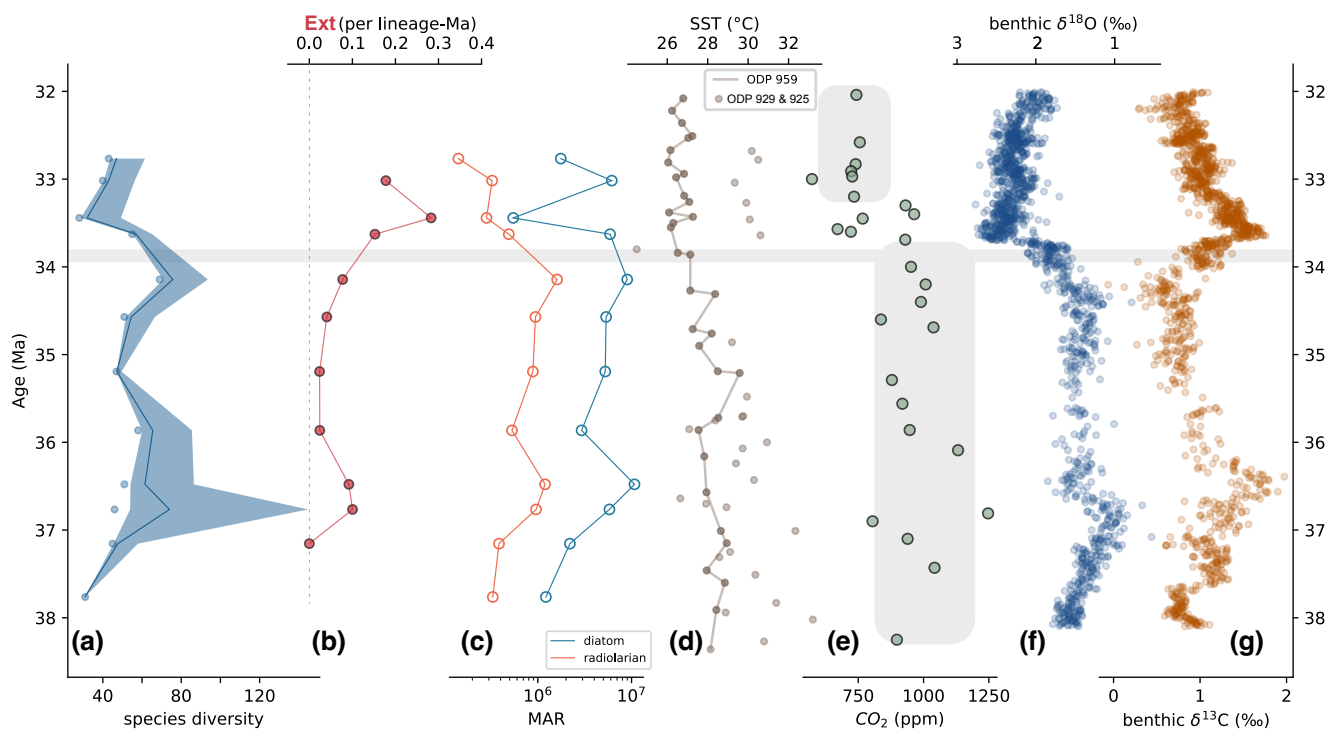
All analyses were performed using Python programming language (Python Software Foundation, version 3.11). Pairwise Spearman correlations and Mann-Whitney U tests were carried out using the `scipy.stats` module (Virtanen et al., 2020). All code used for these analyses is available online in the following GitHub repository:

<https://github.com/oezenvolkan/Ozenetal2026b>.

### 3 Results

#### 3.1 Observed diatom diversity decreases after ~34 Ma

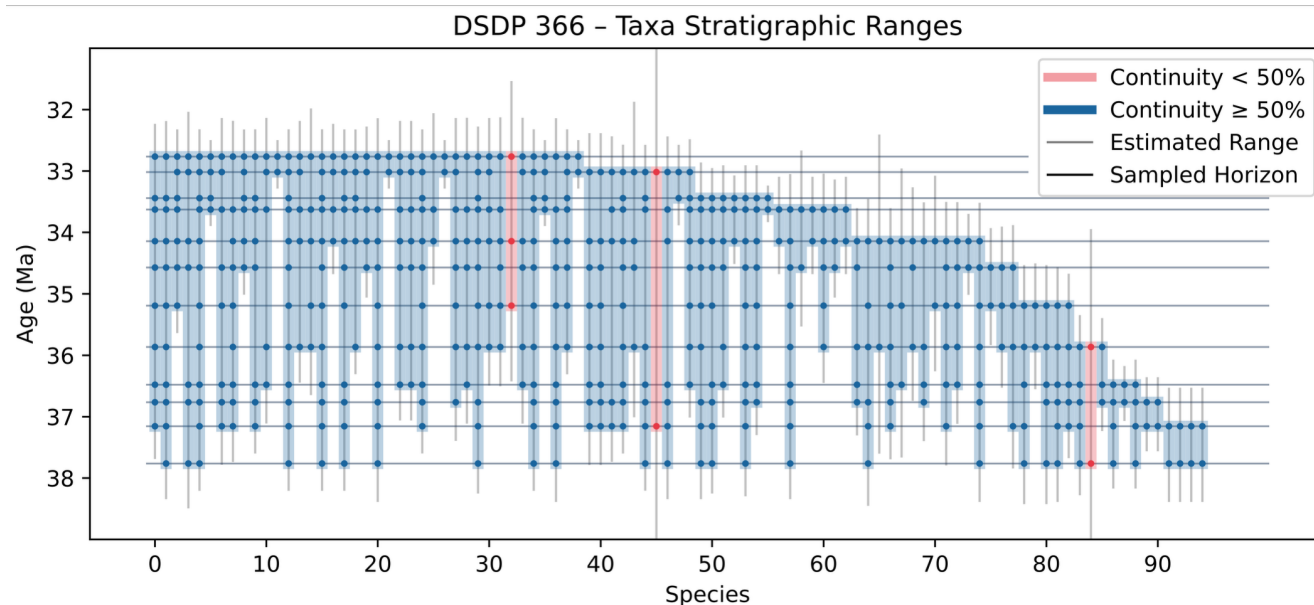
Observed species diversity at DSDP Site 366 remains between 50 and 60 species throughout the late Eocene (Fig. 2a). Diversity approaches its highest at ~34 Ma, at the onset of the Eocene/Oligocene boundary, reaching nearly 80 species. In younger, Oligocene samples, values decrease to levels comparable to those recorded in the oldest samples (~37.8 Ma). Chao1 estimates show a similar overall pattern (Fig. 2a). A notable divergence between observed and estimated diversity values occurs at ~36.8 Ma, where the estimated diversity reaches values comparable to the Chao1 estimate at ~34 Ma.



210 **Figure 2: (a) Diatom diversity (scatter points) with Chao1 diversity estimates (solid line, 95% confidence envelope). (b) Foote**  
**boundary-crosser extinction rates. (c) Diatom and radiolarian accumulation rates (diatom or radiolarian cm<sup>-2</sup> kyr<sup>-1</sup>).**  
**(d) Equatorial Atlantic sea surface temperature (SST) reconstructions: brown datapoints with solid line represent SST values from**  
**ODP Site 959 (after Cramwinckel et al., 2018), while light-brown scatter points show SST values from ODP Sites 925 and 929**  
**(after Liu et al., 2009). (e) Atmospheric CO<sub>2</sub> concentrations (ppm) values across the EOT (from Zhang et al. 2013; Anagnostou et**  
 215 **al. 2020). (f) Global composite benthic foraminiferal δ<sup>18</sup>O and (g) δ<sup>13</sup>C records (from Westerhold et al., 2020).**

### 3.2 Extinction rates rise near the Eocene/Oligocene boundary

Extinction rates remain close to zero throughout the late Eocene, except for a small increase between ~37 and 36.5 Ma (Fig. 2b). The observed taxon ranges during the late Eocene indicate a continuity without substantial turnover (Fig. 3). This trend  
 220 shifts in the latest Eocene, with extinction rates rising from ~34.5 onward, peaking at ~33.5 Ma, and remaining elevated in the Oligocene samples (Fig. 2b).



225 **Figure 3: Taxon ranges for each species observed at DSDP 366, with estimated (see Methods) stratigraphic ranges. Horizontal lines show sampled horizons. In stratigraphic range plots, single-occurrence species are not shown. Taxon range continuity represents the percentage of occurrences of species within their observed ranges.**

### 3.3 Diatom and radiolarian mass accumulation rates

During the Late Eocene, diatom and radiolarian MARs show a similar trend (Fig. 2c). This relationship is also reflected in the diatom-radiolarian (D/R) ratio, which remains nearly constant in the Eocene samples (Fig. S1). Both groups increase in abundance across the Middle- to Late-Eocene transition, reaching a maximum at ~36.5 (Fig. 2c). After this maximum, 230 accumulation rates decline to values similar to those before 37 Ma, then climb modestly again toward 34 Ma, reaching levels comparable to the ~36.5 Ma maximum.

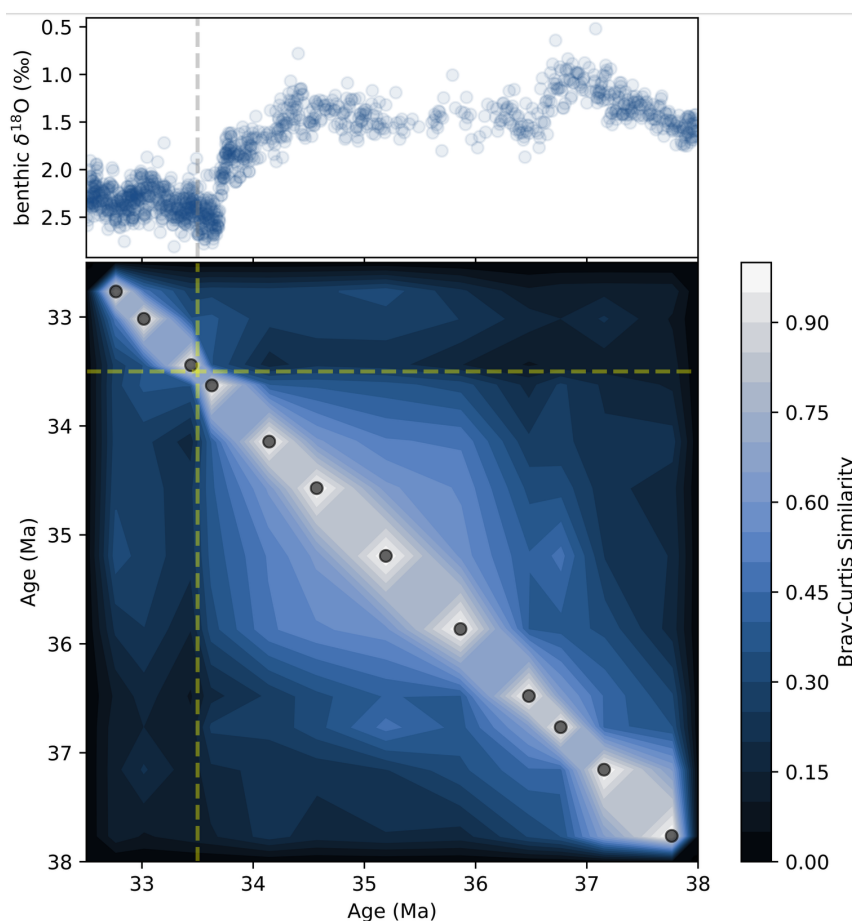
From ~34 Ma onward, the diatom and radiolarian records diverge. Radiolarian accumulation rates decrease into the Early Oligocene, whereas diatom accumulation rates remain relatively stable. A notable exception occurs in a single sample at 235 ~33.5 Ma, where diatom accumulation rates drop to their lowest recorded values.

### 3.4 Diatom community similarity and assemblage dynamics

To examine changes in community composition beyond species diversity and abundance, we calculated community similarity using Bray-Curtis index (Bray and Curtis, 1957; see Methods section 2.5), where values range from 0 (complete 240 dissimilarity) to 1 (complete similarity).



The two samples predating 37 Ma (below ca. 461.5 mbsf) exhibit relatively high self-similarity, with values exceeding 0.6 (Fig. 4). Similarity between these older (>37 Ma) communities and younger late Eocene communities declines sharply. Samples between 37–36 Ma represent communities which have affinities with communities in both older and younger intervals. Within the latest Eocene, after 36 Ma, diatom communities show higher mutual similarity (Fig. 4), though values among Late Eocene samples rarely exceed 0.6. At the E/O, community similarities undergo reorganization. After 34 Ma, similarity between Early Oligocene and Late Eocene samples declines. However, the earliest Oligocene communities retain affinity with their Late Eocene counterparts. The most pronounced shift in community similarity however occurs at 33.5 Ma, and marks a fundamental shift in community composition



250

255

**Figure 4: Global  $\delta^{18}\text{O}$  records and temporal self-similarity of diatom communities.** (Top) Global composite benthic foraminiferal  $\delta^{18}\text{O}$  records spanning the study interval (data from Westerhold et al., 2021). (Bottom) Temporal self-similarity of diatom assemblages at DSDP Site 366. The contour plot displays pair-wise Bray-Curtis similarity values for all sample combinations analyzed. Both axes represent sample age (Ma). Data points (black) along the diagonal mark the analyzed samples, and contours indicate the interpolated similarity values (see scale; 1 = identical communities, 0 = no similarity). Dashed lines mark the phase-shift in diatom community compositions at 33.5 Ma.



To examine assemblage shifts independent of extinction, we compared rank abundances of the most abundant species that are consistently observed across the entire study interval. Around sixty percent of these species shifted rank substantially between the Late Eocene and Early Oligocene (Fig. S2). We quantified these shifts using pairwise Spearman rank correlations of log-transformed abundance values. These correlations are consistent with rank-abundance changes, with within-epoch correlations ( $n = 34$ , Eocene-Eocene and Oligocene-Oligocene) exceeding cross-E/O correlations ( $n = 32$ ), as confirmed by a Mann-Whitney U test ( $U = 340$ ;  $p = 0.00451$ ; Fig. S3). The relative abundances of the dominant diatom genera also shifted across the E/O (Fig. 5). During the Late Eocene, the dominance profile was broadly stable, with the genus *Hemiaulus* being the most abundant group. In the earliest Oligocene, this composition changed as genus *Cestodiscus* became the dominant genus, accompanied by a substantial decrease in the relative abundance of *Hemiaulus* (Fig. 5).

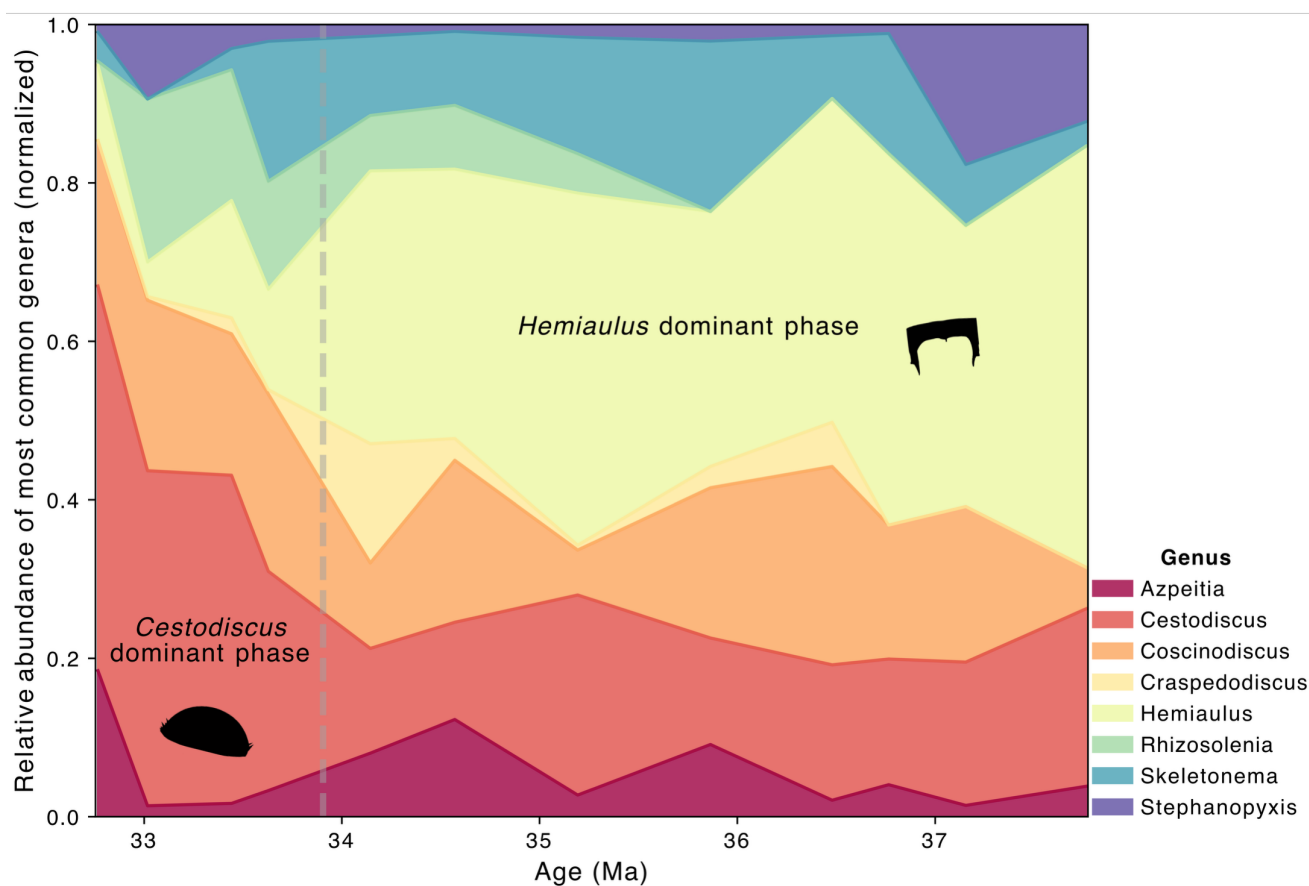


Figure 5: Relative abundance of dominant diatom genera at DSDP Site 366. The figure displays the normalized relative abundances of the most common genera across the study interval. The dashed line marks the Eocene/Oligocene boundary at 33.9 Ma.



## 4 Discussion

The diatom record at DSDP 366 resolves three intervals of ecological change that define the low-latitude response across the Late Eocene-Early Oligocene transition: (1) increasing productivity and emerging community change between 38 and 36  
275 Ma, corresponding to the Middle- to Late-Eocene transition, (2) relative stability from 36 to 34.5 Ma, and (3) the turnover associated with the E/O (34.5 and younger). These intervals illuminate how large-scale climatic and circulation shifts, previously documented in circum-Antarctic regions, manifested in the equatorial Atlantic. Specifically, we assess whether low-latitude diatom communities merely tracked broader paleoceanographic reorganization or if their diversity, productivity, and community structure responded to distinct, local environmental constraints.

### 280 4.1 Tempo and mode of diatom diversity and productivity dynamics across the Eocene/Oligocene Transition

#### 4.1.1 Changes across the Middle-to-Late Eocene transition (38–36 Ma)

Diatom diversity at DSDP Site 366 remains stable between 38 and 36 Ma in raw species counts (Fig. 2a), yet Chao1  
285 diversity estimates rise sharply near 36.8 Ma, coinciding with a shift in community structure (Fig. 4). Similarity values indicate a transitional interval between ~37 and 36 Ma. During this interval, assemblages retain affinities with both older and younger samples but become increasingly self-similar toward the latest Eocene (Fig. 4). Biogenic opal production also intensifies: diatom and radiolarian MARs increase by nearly an order of magnitude and peak around 36.5 Ma (Fig. 2c). Although detailed comparison is difficult due to the low time resolution of our Site 366 data, a broadly comparable increase is recorded in the western equatorial Atlantic, where opal accumulation at ODP Site 925 rises between 38–36 Ma (Fig. S4).  
290 Together, this consistent reorganization of productivity, diversity and community composition suggests that DSDP Site 366 records capture a regional shift in surface ocean conditions in the equatorial Atlantic, likely linked to changes in upwelling intensity and export production during the Middle-to-Late Eocene transition.

The significance of this interval extends beyond the equatorial Atlantic, with parallel changes reported from the Southern Ocean and North Atlantic. Between 38 and 36 Ma, multiple Southern Ocean records show marked increases in productivity,  
295 evidenced by higher biogenic barium accumulation, benthic foraminiferal accumulation and rising opal fluxes (Diester-Haass and Zahn, 1996; Diekmann et al., 2004; Anderson and Delaney, 2005; Rodrigues de Faria et al., 2024; Özen et al., 2025b). Diatom diversity and abundance also increased (Lazarus et al., 2014; Renaudie, 2016; Özen et al., 2025a). In the Indian Ocean sector of the Southern Ocean, nannofossils indicate a shift to a more eutrophic phase (Villa et al., 2014), radiolarians and diatoms undergo taxonomic turnover in the southern high latitudes (Funakawa and Nishi, 2008; Pascher et al., 2015; Özen et al., 2025a) and coccolithophores experienced an ecological shift in the southern Atlantic (Ma et al., 2023).  
300 The North Atlantic also shows elevated opal accumulation within this interval (Witkowski et al., 2021). The temporal alignment of these changes across regions provides essential context for the DSDP 366 diatom record and motivates a key



question: does the eastern equatorial Atlantic diatom record track the propagation of the high-latitude signals and what does it reveal about the degree of coupling between polar and low-latitude ecosystems during the EOT?

305

The coherence of the 38–36 Ma productivity signals suggests a driver that operates at the basin-scale rather than through local factors alone. This interpretation is consistent with benthic foraminiferal  $\delta^{18}\text{O}$  and  $\delta^{13}\text{C}$  records, which were interpreted as marking a transition from thermally homogeneous deep waters to a regime dominated by cold Southern Component Water (SCW) at intermediate depths by ~37.6 Ma (Langton et al., 2016). By ~36.6 Ma, SCW influence expanded into the equatorial Atlantic (Langton et al., 2016) coinciding with peak diatom and radiolarian accumulation at DSDP 366. The changes temporally align with proposed onset of a proto-AMOC around 38 Ma (Borrelli et al., 2014) and with evidence for thermal differentiation in the southern Atlantic (Langton et al., 2016). Ideally positioned to capture this oceanographic reorganization, the eastern equatorial Atlantic likely preserves physical evidence of this reorganization in the form of widespread erosional hiatuses generated by intensified bottom currents in the early Late Eocene (Stein and Faugères, 1989). Recent work shows that deep-sea hiatuses are often linked to major reorganizations of Cenozoic deep-water circulation (Dutkiewicz and Müller, 2022), reinforcing the interpretation that southern-sourced overturning cell expanded northward through the Atlantic during this time.

315

We interpret the increase in biosiliceous accumulation at DSDP Site 366 as the biological fingerprint of this oceanographic reorganization. The near-absence of siliceous microfossils before ~38 Ma partially reflects diagenesis (Lancelot et al., 1978; Fenner, 1982), but it may also indicate that diatom production remained below the threshold needed for sustained export and preservation in the water column (e.g., Takahashi, 1991; Kiørboe, 1993; Jackson, 2001). The increasing influence of SCW (Langton et al., 2016) likely raised the silica saturation of deep waters, facilitating biogenic opal to accumulate even before peak production was reached at 36.6 Ma.

320

#### 325 **4.1.2 Late Eocene relative stability (36–34.5 Ma)**

The latest Eocene interval at DSDP 366 (~36–34.5 Ma) marks a phase of relative stability in both diatom diversity and community structure. Diversity values vary little (Fig. 2a), communities become more self-similar (Fig. 4), and extinction rates remain close to zero (Fig. 2b). This stability is not unique to DSDP Site 366. In the sub-Antarctic Atlantic, diatom diversity and community composition show a similar steady pattern (Özen et al., 2025a) following the major shifts of the Middle- to Late-Eocene transition. In the arc of Late Eocene change, this stability stands out as the “Calm Before the Storm” that led into the Eocene/Oligocene shift (Prothero, 1994, p. 151).

330

Throughout the Eocene section, diatom and radiolarian MARs track each other closely and diatom-to-radiolarian (D/R) ratio remains stable (Fig. 2c; Fig. S1). Experimental and sediment studies show that diatom assemblages are more sensitive to dissolution than radiolarians (Lisitzin, 1972; Johnson, 1974; Lazarus, 2011), and a selective dissolution effect tends to lower

335



D/R ratio. The use of D/R as a simple preservation and productivity proxy in other EOT sections provides further context (e.g., Moore et al., 2014; Pascher et al., 2015). Thus, the nearly constant D/R ratio before 34 Ma argues against a progressive increase in differential dissolution at DSDP Site 366 and supports the view that the Late Eocene diversity signal is primarily ecological.

340

Records across the Southern Ocean and Atlantic indicate the ~36–34 Ma interval as a period of stable, relatively low productivity phase following the large environmental and evolutionary changes that unfolded between 38 and 36 Ma. In the southwest Pacific, radiolarian diversity and diatom abundance drop at 36 Ma, remaining low until the E/O (Pascher et al., 2015). Southern Ocean and sub-Antarctic sites (ODP 689, 748, 1090; Fig. 1) show similar shift to a lower base level in bio-  
barium, diatom, opal, and benthic foraminiferal accumulation rates (Diester-Haass and Zahn, 1996; Diekmann et al., 2004; Anderson and Delaney, 2005; Rodrigues de Faria et al., 2024; Özen et al., 2025b). This pattern extends to the western equatorial Atlantic, where ODP Site 925 records a near shutdown of biogenic opal burial between 36 and 34 Ma (Nilsen et al., 2003; Fig. S4). Such widespread coherence hints at a common oceanographic regime in the latest Eocene, potentially conditioned by the deepening of the Tasman Gateway and a strengthening circum-Antarctic circulation (Stickley et al., 2004; Borrelli et al., 2014; Rodrigues de Faria et al., 2024).

350

#### 4.1.3 Changes surrounding the Eocene/Oligocene boundary: 34.5 Ma onwards

The late Eocene to Early Oligocene interval at DSDP Site 366 records a major ecological shift in diatom communities. From ~34.5 Ma on, extinction rates rise and peak near ~33.5 Ma, and diatom diversity drops that does not recover to Late Eocene levels (Fig. 2a-b). Diatom productivity reaches a second maximum near 34 Ma, and radiolarian productivity peaks at about the same time (Fig. 2c). The strongest ecological transition occurs at around 33.5 Ma, when extinction, diversity and community similarity show threshold-like shifts (Fig. 2a-b and 4), consistent with earlier work from the region (Corliss et al., 1984; Fenner, 1982).

355

A central feature of this transition is the divergence between diatom and radiolarian productivity. From ~34 Ma onward, radiolarian productivity declines and shows no clear recovery in the earliest Oligocene (Fig. 2c). In contrast, diatom productivity remains comparable to Late Eocene values, interrupted only by a pronounced minimum at ~33.5 Ma before rebounding to higher levels (Fig. 2c). Our sampling resolution does not resolve when ~33.5 Ma diatom MAR minimum begins within the 34–33 Ma interval and how abrupt it is. However, a pronounced transient productivity low near ~33.5 Ma, the Early Oligocene Glacial Maximum (EOGM) (or Oi-1; see Hutchinson et al., 2021 and references therein for nomenclature), is a well-documented feature of the tropical marine record (e.g., Griffith et al., 2010; Erhardt et al., 2013; Moore et al., 2014). In the eastern equatorial Pacific, barite and opal accumulation rates show a transient minimum linked to upper-ocean reorganization and thermocline deepening, while synchronous peaks in benthic foraminiferal accumulation rates likely reflect increased deep-water oxygenation (Moore et al., 2014). Although our sampling resolution limits the precise

365



temporal extent of this minimum at DSDP Site 366, this coherence between eastern equatorial Pacific and Atlantic records  
370 might suggest a tropical response to high-latitude forcing and offers a testable basis for linking these ecosystems to the likely  
propagated effects of Southern Ocean gateway evolution, as emphasized for the eastern equatorial Pacific by Moore et al.  
(2014).

The recovery in diatom productivity following the transient minimum at ~33.5 Ma is not matched by a recovery in diversity.  
375 Diversity remains low even as diatom productivity returns to higher levels (Fig. 2a-c). Extinction rates were already rising in  
the latest Eocene, suggesting that the diversity loss in the earliest Oligocene reflects a true biological signal rather than an  
artifact of reduced abundance in diatoms, consistent with earlier studies (Corliss et al., 1984). This contrast suggests an  
environmental filtering favoring a subset of taxa capable of sustaining productivity comparable to levels seen across the Late  
Eocene.

380

This environmental filtering is unlikely to be driven by surface cooling in the tropical Atlantic. Surface temperature change  
is often linked to plankton overturning in the paleorecord (e.g., Trubovitz et al., 2020; Özen et al., 2025a) but tropical  
Atlantic SST records suggest relatively stable surface ocean temperatures across the boundary (e.g., Liu et al., 2009;  
Cramwinckel et al., 2018; Fig. 2d). Therefore, the signal at DSDP 366 appears more consistent with (1) changes in upper-  
385 ocean stratification and thermocline depth, (2) associated shifts in nutrient supply into the sunlit zone, (3) changes in deep-  
water expansion. Under this set of mechanisms, sustained diatom productivity alongside constantly declining radiolarian  
productivity can arise if mixed-layer stability and thermocline depth change to favor a narrower set of diatom taxa, while  
simultaneously reducing the habitat for radiolarian fauna adapted to the warm, thick mixed-layer conditions of the Late  
Eocene (e.g., Lazarus, 2005).

390

This structural shift is evident in diatom community evolution and dominant assemblage profiles. In the Late Eocene at  
DSDP Site 366, the assemblage is dominated by *Hemiaulus* (Fig. 5), a genus plausibly associated with stable, stratified  
upper-ocean conditions (e.g., Guillard and Kilham, 1977; Kemp et al., 2000; Kemp and Villareal, 2018). With the onset of  
the Oligocene, the assemblage shifts to a genus *Cestodiscus*-dominated phase (Fig. 5; see also Corliss et al., 1984; Fenner,  
395 1986). An increase in *Cestodiscus* abundance is a recurrent feature of the E/O records at the southern high latitudes,  
especially at Antarctic-proximal sites (ODP 689 and 748, Fig. 1; Özen et al., 2025a), where the earliest Oligocene conditions  
are generally interpreted as more strongly mixed, eutrophic conditions with the Oligocene cooling, as evidence by numerous  
studies (e.g., Diester-Haass and Zahn, 1996; Salamy and Zachos, 1999; Villa et al., 2014; Rodrigues De Faria et al., 2024;  
Özen et al., 2025b). The link between the rise of genus *Cestodiscus* and increasing intensity of surface currents, mixing and  
400 nutrient availability has already been suggested by Fenner (1986), and later data align with her interpretations (Özen et al.,  
2025a). The appearance of similar dominance shifts at DSDP Site 366, together with decline of genus *Hemiaulus* into the  
earliest Oligocene is consistent with a change in upper-ocean mixing and nutrient supply affecting low-latitude ecosystems,



potentially reflecting the imprints of wider oceanographic reorganization associated with Antarctic glaciation and Southern Ocean gateway evolution.

405

Species-level community similarity trends also support this view. While the immediate post-E/O assemblages retain Eocene affinities, diatom communities cross an ecological threshold at ~33.5 Ma where similarity values show a phase shift (Fig. 4). This transition is not explained by increasing extinction rates, and thus species loss in the earliest Oligocene, as taxa that persist across the study interval reorganize substantially in relative abundance, producing marked reshuffling of the rank-abundance structure (Fig. S2). Moreover, species rank abundance profiles are more similar within epochs than across the E/O suggesting that Oligocene conditions favored a new set of niche selecting diatoms. Together, these patterns indicate a dynamic re-sorting of community structure consistent with changing physical oceanographic conditions in the earliest Oligocene eastern equatorial Atlantic, potentially involving shifts in stratification and nutrient delivery under global cooling. This interpretation is consistent with recent evidence from the western equatorial Atlantic, where planktonic foraminiferal assemblages document a substantial restructuring of ocean stratification across the E/O, specifically characterized by the collapse of the stable oligotrophic surface mixed layer and the expansion of sub-thermocline habitats (Woodhouse et al., 2025).

410  
415

## Conclusion

The EOT (~38-32 Ma) at DSDP Site 366 captures a fundamental ecological restructuring in low-latitude diatom communities. While extinction rates remained low through most of the Eocene, they rose sharply in the earliest Oligocene, marking a threshold event at ~33.5 Ma that coincided with a significant change in community composition. Unlike high-latitude plankton, where SST changes have been linked to extinction events, our results indicate that in the equatorial Atlantic, oceanographic processes, particularly an inferred collapse of the stratified upper ocean niche, likely played a dominant role in shaping diatom assemblages. The relative stability of diatom productivity in the earliest Oligocene, coupled with a sharp decline in radiolarians and reduced diatom diversity, suggests that the EOT was characterized not by a uniform productivity collapse but by a structural shift in upper ocean stratification selecting taxa over stability adapted groups. This study provides direct evidence that low-latitude diatom communities underwent substantial reorganization, not simply as a response to temperature change, but as part of a broader transformation in ocean circulation and the development of temperature gradients driven by high-latitude climatic and oceanographic shifts propagating across ocean basins.

425

## 430 Author contributions

VÖ collected and analyzed the data and drafted the manuscript. All authors contributed to revision and editing of the final version.



### Competing interests

The contact author has declared that none of the authors has any competing interests.

### 435 Acknowledgements

We thank Sylvia Dietze (MfN Berlin) for her assistance with sample preparation.

### Financial support

This study was funded by the Federal Ministry of Education and Research (BMBF) under the “Make our Planet Great Again – German Research Initiative”, grant number 57429681, implemented by the German Academic Exchange Service (DAAD).

### 440 References

Anagnostou, E., John, E. H., Babila, T. L., Sexton, P. F., Ridgwell, A., Lunt, D. J., Pearson, P. N., Chalk, T. B., Pancost, R. D., and Foster, G. L.: Proxy evidence for state-dependence of climate sensitivity in the Eocene greenhouse, *Nat Commun*, 11, 4436, <https://doi.org/10.1038/s41467-020-17887-x>, 2020.

445 Anderson, L. D. and Delaney, M. L.: Middle Eocene to early Oligocene paleoceanography from Agulhas Ridge, Southern Ocean (Ocean Drilling Program Leg 177, Site 1090), *Paleoceanography*, 20, 2004PA001043, <https://doi.org/10.1029/2004PA001043>, 2005.

Baldauf, J. G., Monjanel, A. L.: An Oligocene Diatom Biostratigraphy for the Labrador Sea: DSDP Site 112 and ODP Hole  
450 647A. *Proceedings of the Ocean Drilling Program, 105 Scientific Results. Ocean Drilling Program.* <https://doi.org/10.2973/odp.proc.sr.105.129.1989>, 1989.

Baldauf, J. G. and Barron, J. A.: Evolution of Biosiliceous Sedimentation Patterns — Eocene Through Quaternary: Paleoceanographic Response to Polar Cooling, in: *Geological History of the Polar Oceans: Arctic versus Antarctic*, edited  
455 by: Bleil, U. and Thiede, J., Springer Netherlands, Dordrecht, 575–607, [https://doi.org/10.1007/978-94-009-2029-3\\_32](https://doi.org/10.1007/978-94-009-2029-3_32), 1990.

Barker, P. F.: Scotia Sea regional tectonic evolution: implications for mantle flow and palaeocirculation, *Earth-Science Reviews*, 55, 1–39, [https://doi.org/10.1016/S0012-8252\(01\)00055-1](https://doi.org/10.1016/S0012-8252(01)00055-1), 2001.

460



- Barron, J.A. and Baldauf, J.G.: Tertiary cooling steps and paleoproductivity as reflected by diatoms and biosiliceous sediments. In: W.H. Berger, V.S. Smetacek and G. Wefer (Editors), *Productivity of the Ocean: Present and Past*. Wiley, New York, pp. 341-354, 1989.
- 465 Barron, J. A., Stickley, C. E., and Bukry, D.: Paleooceanographic, and paleoclimatic constraints on the global Eocene diatom and silicoflagellate record, *Palaeogeography, Palaeoclimatology, Palaeoecology*, 422, 85–100, <https://doi.org/10.1016/j.palaeo.2015.01.015>, 2015.
- Behrenfeld, M. J., Halsey, K. H., Boss, E., Karp-Boss, L., Milligan, A. J., and Peers, G.: Thoughts on the evolution and ecological niche of diatoms, *Ecological Monographs*, 91, e01457, <https://doi.org/10.1002/ecm.1457>, 2021.
- 470
- Borrelli, C., Cramer, B. S., and Katz, M. E.: Bipolar Atlantic deepwater circulation in the middle-late Eocene: Effects of Southern Ocean gateway openings, *Paleoceanography*, 29, 308–327, <https://doi.org/10.1002/2012PA002444>, 2014.
- 475 Bray, J. R. and Curtis, J. T.: An ordination of the upland forest communities of southern Wisconsin, *Ecological Monographs*, 27, 326–349, 1957.
- Chao, A.: Nonparametric estimation of the number of classes in a population, *Scandinavian Journal of statistics*, 265–270, 1984.
- 480
- Corliss, B. H., Aubry, M.-P., Berggren, W. A., Fenner, J. M., Keigwin, L. D., and Keller, G.: The Eocene/Oligocene Boundary Event in the Deep Sea, *Science*, 226, 806–810, <https://doi.org/10.1126/science.226.4676.806>, 1984.
- Cortese, G., Gersonde, R., Hillenbrand, C.-D., and Kuhn, G.: Opal sedimentation shifts in the World Ocean over the last 15 Myr, *Earth and Planetary Science Letters*, 224, 509–527, <https://doi.org/10.1016/j.epsl.2004.05.035>, 2004.
- 485
- Coxall, H. K., Wilson, P. A., Pälike, H., Lear, C. H., and Backman, J.: Rapid stepwise onset of Antarctic glaciation and deeper calcite compensation in the Pacific Ocean, *Nature*, 433, 53–57, <https://doi.org/10.1038/nature03135>, 2005.
- 490 Crampton, J. S., Cody, R. D., Levy, R., Harwood, D., McKay, R., and Naish, T. R.: Southern Ocean phytoplankton turnover in response to stepwise Antarctic cooling over the past 15 million years, *Proc. Natl. Acad. Sci. U.S.A.*, 113, 6868–6873, <https://doi.org/10.1073/pnas.1600318113>, 2016.



495 Cramwinckel, M. J., Huber, M., Kocken, I. J., Agnini, C., Bijl, P. K., Bohaty, S. M., Frieling, J., Goldner, A., Hilgen, F. J.,  
Kip, E. L., Peterse, F., Van Der Ploeg, R., Röhl, U., Schouten, S., and Sluijs, A.: Synchronous tropical and polar temperature  
evolution in the Eocene, *Nature*, 559, 382–386, <https://doi.org/10.1038/s41586-018-0272-2>, 2018.

De La Rocha, C. L. and Passow, U.: The Biological Pump, in: *Treatise on Geochemistry*, Elsevier, 93–122,  
<https://doi.org/10.1016/B978-0-08-095975-7.00604-5>, 2014.

500

Diekmann, B., Kuhn, G., Gersonde, R., and Mackensen, A.: Middle Eocene to early Miocene environmental changes in the  
sub-Antarctic Southern Ocean: evidence from biogenic and terrigenous depositional patterns at ODP Site 1090, *Global and  
Planetary Change*, 40, 295–313, <https://doi.org/10.1016/j.gloplacha.2003.09.001>, 2004.

505 Diester-Haass, L. and Zahn, R.: Eocene-Oligocene transition in the Southern Ocean: History of water mass circulation and  
biological productivity, *Geol*, 24, 163, [https://doi.org/10.1130/0091-7613\(1996\)024%253C0163:eotits%253E2.3.co;2](https://doi.org/10.1130/0091-7613(1996)024%253C0163:eotits%253E2.3.co;2), 1996.

Dutkiewicz, A. and Müller, R. D.: Deep-sea hiatuses track the vigor of Cenozoic ocean bottom currents, *Geology*, 50, 710–  
715, <https://doi.org/10.1130/G49810.1>, 2022.

510

Erhardt, A. M., Pälike, H., and Paytan, A.: High-resolution record of export production in the eastern equatorial Pacific  
across the Eocene-Oligocene transition and relationships to global climatic records, *Paleoceanography*, 28, 130–142,  
<https://doi.org/10.1029/2012PA002347>, 2013.

515 Elsworth, G., Galbraith, E., Halverson, G., and Yang, S.: Enhanced weathering and CO<sub>2</sub> drawdown caused by latest Eocene  
strengthening of the Atlantic meridional overturning circulation, *Nature Geosci*, 10, 213–216,  
<https://doi.org/10.1038/ngeo2888>, 2017.

520 Eppley, R. W. and Peterson, B. J.: Particulate organic matter flux and planktonic new production in the deep ocean, *Nature*,  
282, 677–680, <https://doi.org/10.1038/282677a0>, 1979.

Fenner, J.: Diatoms in the Eocene and Oligocene sediments off N.W. Africa, their stratigraphic and paleogeographic  
occurrences. Dissertation zur Erlangung des Doktorgrades der Mathematisch Naturwissenschaftlichen Fakultät der Christian-  
Albrechts-Universität zu Kiel, Kiel (in German), 1982.

525

Fenner, J.: Eocene-Oligocene Planktic Diatom Stratigraphy in the Low Latitudes and the High Southern Latitudes,  
*Micropaleontology*, 30, 319, <https://doi.org/10.2307/1485708>, 1984.



530 Fenner, J.: Late Cretaceous to Oligocene planktic diatoms. In: Bolli, H.M., Saunders, J.B., and Perch-Nielsen, K. (eds.),  
Plankton Stratigraphy. Cambridge University Press, pp. 713-762, 1985.

Fenner, J.: Information from Diatom Analysis Concerning the Eocene-Oligocene Boundary, in: Developments in  
Palaeontology and Stratigraphy, vol. 9, Elsevier, 283–287, [https://doi.org/10.1016/S0920-5446\(08\)70131-6](https://doi.org/10.1016/S0920-5446(08)70131-6), 1986.

535 Foote, M.: Origination and extinction components of taxonomic diversity: General problems, *Paleobiology*, 26, 74–102,  
<https://doi.org/10.1017/S0094837300026890>, 2000.

540 Galeotti, S., Bijl, P., Brinkuis, H., M. DeConto, R., Escutia, C., Florindo, F., G.W. Gasson, E., Francis, J., Hutchinson, D.,  
Kennedy-Asser, A., Lanci, L., Sauermilch, I., Sluijs, A., and Stocchi, P.: The Eocene-Oligocene boundary climate transition:  
an Antarctic perspective, in: *Antarctic Climate Evolution*, Elsevier, 297–361, <https://doi.org/10.1016/B978-0-12-819109-5.00009-8>, 2022.

Gladenkov, A.: Bipolar distribution of some earliest Oligocene marine diatoms, *Nova Hedwigia*, 143, 337–368,  
<https://doi.org/10.1127/1438-9431/2014/017>, 2014.

545

Griffith, E., Calhoun, M., Thomas, E., Averyt, K., Erhardt, A., Bralower, T., Lyle, M., Olivarez-Lyle, A., and Paytan, A.:  
Export productivity and carbonate accumulation in the Pacific Basin at the transition from a greenhouse to icehouse climate  
(late Eocene to early Oligocene): E-O Paleoproductivity, *Paleoceanography*, 25, <https://doi.org/10.1029/2010PA001932>,  
2010.

550

Guillard, R.R.L., Kilham, P.: The ecology of marine planktonic diatoms. In: Werner, D. (Ed.), *The Biology of Diatoms*.  
University of California Press. Berkeley. pp. 372--346, 1977.

555 Hutchinson, D. K., Coxall, H. K., Lunt, D. J., Steinthorsdottir, M., De Boer, A. M., Baatsen, M., Von Der Heydt, A., Huber,  
M., Kennedy-Asser, A. T., Kunzmann, L., Ladant, J.-B., Lear, C. H., Moraweck, K., Pearson, P. N., Piga, E., Pound, M. J.,  
Salzmann, U., Scher, H. D., Sijp, W. P., Śliwińska, K. K., Wilson, P. A., and Zhang, Z.: The Eocene–Oligocene transition: a  
review of marine and terrestrial proxy data, models and model–data comparisons, *Clim. Past*, 17, 269–315,  
<https://doi.org/10.5194/cp-17-269-2021>, 2021.

560 Jackson, G. A.: Effect of coagulation on a model planktonic food web, *Deep Sea Research Part I: Oceanographic Research  
Papers*, 48, 95–123, [https://doi.org/10.1016/S0967-0637\(00\)00040-6](https://doi.org/10.1016/S0967-0637(00)00040-6), 2001.

Johnson, T. C.: The dissolution of siliceous microfossils in surface sediments of the eastern tropical Pacific, *Deep Sea Research and Oceanographic Abstracts*, 21, 851–864, [https://doi.org/10.1016/0011-7471\(74\)90004-7](https://doi.org/10.1016/0011-7471(74)90004-7), 1974.

565

Jones, E. J. W., Cande, S. C., and Spathopoulos, F.: Evolution of a major oceanographic pathway: the equatorial Atlantic, *SP*, 90, 199–213, <https://doi.org/10.1144/GSL.SP.1995.090.01.12>, 1995.

Kemp, A. E. S., Pike, J., Pearce, R. B., and Lange, C. B.: The “Fall dump” — a new perspective on the role of a “shade  
570 flora” in the annual cycle of diatom production and export flux, *Deep Sea Research Part II: Topical Studies in Oceanography*, 47, 2129–2154, [https://doi.org/10.1016/S0967-0645\(00\)00019-9](https://doi.org/10.1016/S0967-0645(00)00019-9), 2000.

Kemp, A. E. S. and Villareal, T. A.: The case of the diatoms and the muddled mandalas: Time to recognize diatom  
575 adaptations to stratified waters, *Progress in Oceanography*, 167, 138–149, <https://doi.org/10.1016/j.pocean.2018.08.002>, 2018.

Kennett, J. P.: Cenozoic evolution of Antarctic glaciation, the circum-Antarctic Ocean, and their impact on global  
paleoceanography, *Journal of Geophysical Research (1896-1977)*, 82, 3843–3860,  
580 <https://doi.org/10.1029/JC082i027p03843>, 1977.

Kjørboe, T.: Turbulence, Phytoplankton Cell Size, and the Structure of Pelagic Food Webs, in: *Advances in Marine Biology*,  
vol. 29, Elsevier, 1–72, [https://doi.org/10.1016/S0065-2881\(08\)60129-7](https://doi.org/10.1016/S0065-2881(08)60129-7), 1993.

Kwon, E. Y., Primeau, F., and Sarmiento, J. L.: The impact of remineralization depth on the air–sea carbon balance, *Nature  
585 Geosci*, 2, 630–635, <https://doi.org/10.1038/ngeo612>, 2009.

Lancelot, Y., Seibold, E., and et al.: *Initial Reports of the Deep Sea Drilling Project*, 41, U.S. Government Printing Office,  
<https://doi.org/10.2973/dsdp.proc.41.1978>, 1978.

590 Langton, S. J., Rabideaux, N. M., Borrelli, C., and Katz, M. E.: Southeastern Atlantic deep-water evolution during the late-  
middle Eocene to earliest Oligocene (Ocean Drilling Program Site 1263 and Deep Sea Drilling Project Site 366), *Geosphere*,  
12, 1032–1047, <https://doi.org/10.1130/GES01268.1>, 2016.

Lazarus, D.: An improved cover-slip holder for preparing microslides of randomly distributed particles, *Journal of  
595 Sedimentary Research*, 64, 686–0, <https://doi.org/10.2110/jsr.64.686>, 1994.



- Lazarus, D., Barron, J., Renaudie, J., Diver, P., and Türke, A.: Cenozoic Planktonic Marine Diatom Diversity and Correlation to Climate Change, *PLoS ONE*, 9, e84857, <https://doi.org/10.1371/journal.pone.0084857>, 2014.
- 600 Lazarus, D. B.: The deep-sea microfossil record of macroevolutionary change in plankton and its study, *SP*, 358, 141–166, <https://doi.org/10.1144/SP358.10>, 2011.
- Lear, C. H., Bailey, T. R., Pearson, P. N., Coxall, H. K., and Rosenthal, Y.: Cooling and ice growth across the Eocene-Oligocene transition, *Geol*, 36, 251, <https://doi.org/10.1130/G24584A.1>, 2008.
- 605 Lisitzin, A. P.: Sedimentation in the World Ocean, *SEPM Special Publications*, *SEPM Society for Sedimentary Geology*, 17, 1972.
- Liu, Z., Pagani, M., Zinniker, D., DeConto, R., Huber, M., Brinkhuis, H., Shah, S. R., Leckie, R. M., and Pearson, A.:  
610 Global Cooling During the Eocene-Oligocene Climate Transition, *Science*, 323, 1187–1190, <https://doi.org/10.1126/science.1166368>, 2009.
- Magurran, Anne E.: *Measuring Biological Diversity*, Wiley, 2004.
- 615 Mann, H. B. and Whitney, D. R.: On a Test of Whether one of Two Random Variables is Stochastically Larger than the Other, *Ann. Math. Statist.*, 18, 50–60, <https://doi.org/10.1214/aoms/1177730491>, 1947.
- Marshall, C. R.: Confidence intervals on stratigraphic ranges with nonrandom distributions of fossil horizons, *Paleobiology*, 23, 165–173, <https://doi.org/10.1017/s0094837300016766>, 1997.
- 620 Miskell, K. J., Brass, G. W., and Harrison, C. G. A.: Global Patterns in Opal Deposition from Late Cretaceous Late Miocene, *AAPG Bulletin*, 69, <https://doi.org/10.1306/AD462B41-16F7-11D7-8645000102C1865D>, 1985.
- Moore, T. C.: Method of randomly distributing grains for microscopic examination, *J. Sediment. Res.*, 43,  
625 <https://doi.org/10.1306/74d728ba-2b21-11d7-8648000102c1865d>, 1973.
- Moore, T. C., Wade, B. S., Westerhold, T., Erhardt, A. M., Coxall, H. K., Baldauf, J., and Wagner, M.: Equatorial Pacific productivity changes near the Eocene-Oligocene boundary, *Paleoceanography*, 29, 825–844, <https://doi.org/10.1002/2014PA002656>, 2014.



630

Nilsen, E. B., Anderson, L. D., and Delaney, M. L.: Paleoproductivity, nutrient burial, climate change and the carbon cycle in the western equatorial Atlantic across the Eocene/Oligocene boundary, *Paleoceanography*, 18, 2002PA000804, <https://doi.org/10.1029/2002PA000804>, 2003.

635 Nowicki, M., DeVries, T., and Siegel, D. A.: Quantifying the Carbon Export and Sequestration Pathways of the Ocean's Biological Carbon Pump, *Global Biogeochemical Cycles*, 36, e2021GB007083, <https://doi.org/10.1029/2021GB007083>, 2022.

Özen, V., Renaudie, J., and Lazarus, D.: Unraveling Southern Ocean Diatom Diversity Across the Eocene/Oligocene  
640 Transition, [preprint: <https://doi.org/10.31223/X50N1B>], *Journal of Micropaleontology*, accepted, 2026.

Özen, V., Renaudie, J., Lazarus, D., and Rodrigues De Faria, G.: Increasing opal productivity in the Late Eocene Southern Ocean: Evidence for increased carbon export preceding the Eocene-Oligocene glaciation, *Clim. Past*, 21, 2283–2297, <https://doi.org/10.5194/cp-21-2283-2025>, 2025a.

645

Özen, V., Renaudie, J., & Lazarus, D. (2026). Özen et al Extinction, Turnover, and the Reorganization of Diatom Communities Across the Eocene-Oligocene Boundary: Equatorial Atlantic Perspective. Zenodo. <https://doi.org/10.5281/zenodo.18723713>

650 Prothero, D. R.: *The Eocene-Oligocene transition: Paradise lost*, Columbia University Press, New York, 291 pp., 1994.

Rabosky, D. L. and Sorhannus, U.: Diversity dynamics of marine planktonic diatoms across the Cenozoic, *Nature*, 457, 183–186, <https://doi.org/10.1038/nature07435>, 2009.

655 Ragueneau, O., Tréguer, P., Leynaert, A., Anderson, R. F., Brzezinski, M. A., DeMaster, D. J., Dugdale, R. C., Dymond, J., Fischer, G., François, R., Heinze, C., Maier-Reimer, E., Martin-Jézéquel, V., Nelson, D. M., and Quéguiner, B.: A review of the Si cycle in the modern ocean: recent progress and missing gaps in the application of biogenic opal as a paleoproductivity proxy, *Global and Planetary Change*, 26, 317–365, [https://doi.org/10.1016/S0921-8181\(00\)00052-7](https://doi.org/10.1016/S0921-8181(00)00052-7), 2000.

660 Ragueneau, O., Schultes, S., Bidle, K., Claquin, P., and Moriceau, B.: Si and C interactions in the world ocean: Importance of ecological processes and implications for the role of diatoms in the biological pump, *Global Biogeochemical Cycles*, 20, 2006GB002688, <https://doi.org/10.1029/2006GB002688>, 2006.



665 Renaudie, J.: Quantifying the Cenozoic marine diatom deposition history: links to the C and Si cycles, *Biogeosciences*, 13, 6003–6014, <https://doi.org/10.5194/bg-13-6003-2016>, 2016.

Renaudie, J. and Lazarus, D. B.: On the accuracy of paleodiversity reconstructions: a case study in Antarctic Neogene radiolarians, *Paleobiology*, 39, 491–509, <https://doi.org/10.1666/12016>, 2013.

670 Richardson, T. L., Cullen, J. J., Kelley, D. E., and Lewis, M. R.: Potential contributions of vertically migrating *Rhizosolenia* to nutrient cycling and new production in the open ocean, *J Plankton Res*, 20, 219–241, <https://doi.org/10.1093/plankt/20.2.219>, 1998.

675 Rodrigues De Faria, G., Lazarus, D., Renaudie, J., Stammeier, J., Özen, V., and Struck, U.: Late Eocene to early Oligocene productivity events in the proto-Southern Ocean and correlation to climate change, *Clim. Past*, 20, 1327–1348, <https://doi.org/10.5194/cp-20-1327-2024>, 2024.

Schumacher, S. and Lazarus, D.: Regional differences in pelagic productivity in the late Eocene to early Oligocene—a comparison of southern high latitudes and lower latitudes, *Palaeogeography, Palaeoclimatology, Palaeoecology*, 214, 243–  
680 263, [https://doi.org/10.1016/S0031-0182\(04\)00424-9](https://doi.org/10.1016/S0031-0182(04)00424-9), 2004.

Siegel, D. A., DeVries, T., Cetinić, I., and Bisson, K. M.: Quantifying the Ocean’s Biological Pump and Its Carbon Cycle Impacts on Global Scales, *Annu. Rev. Mar. Sci.*, 15, 329–356, <https://doi.org/10.1146/annurev-marine-040722-115226>, 2023.

685

Spearman, C.: The Proof and Measurement of Association between Two Things, *The American Journal of Psychology*, 15, 72, <https://doi.org/10.2307/1412159>, 1904.

690 Stein, R. and Faugères, J.: Sedimentological and geochemical characteristics of the Upper Cretaceous and Lower Tertiary sediments at Site 661 (eastern equatorial Atlantic) and their paleoenvironmental significance. In: Ruddiman, W; Sarnthein, M; et al. (eds.), *Proceedings of the Ocean Drilling Program, Scientific Results*, College Station, TX (Ocean Drilling Program), 108, 297–309, <https://doi.org/10.2973/odp.proc.sr.108.135.1989>, 1989.

695 Stickley, C. E., Brinkhuis, H., Schellenberg, S. A., Sluijs, A., Röhl, U., Fuller, M., Grauert, M., Huber, M., Warnaar, J., and Williams, G. L.: Timing and nature of the deepening of the Tasmanian Gateway, *Paleoceanography*, 19, 2004PA001022, <https://doi.org/10.1029/2004PA001022>, 2004.



700 Straume, E. O., Nummelin, A., Gaina, C., and Nisancioglu, K. H.: Climate transition at the Eocene-Oligocene influenced by bathymetric changes to the Atlantic-Arctic oceanic gateways, *PNAS*, 119, e2115346119, <https://doi.org/10.1073/pnas.2115346119>, 2022.

Takahashi, K.: Radiolaria : flux, ecology, and taxonomy in the Pacific and Atlantic, Woods Hole Oceanographic Institution, Woods Hole, MA, <https://doi.org/10.1575/1912/408>, 1991.

705 Tréguer, P., Bowler, C., Moriceau, B., Dutkiewicz, S., Gehlen, M., Aumont, O., Bittner, L., Dugdale, R., Finkel, Z., Iudicone, D., Jahn, O., Guidi, L., Lasbleiz, M., Leblanc, K., Levy, M., and Pondaven, P.: Influence of diatom diversity on the ocean biological carbon pump, *Nature Geosci*, 11, 27–37, <https://doi.org/10.1038/s41561-017-0028-x>, 2018.

710 Tréguer, P. J., Sutton, J. N., Brzezinski, M., Charette, M. A., Devries, T., Dutkiewicz, S., Ehlert, C., Hawkings, J., Leynaert, A., Liu, S. M., Llopis Monferrer, N., López-Acosta, M., Maldonado, M., Rahman, S., Ran, L., and Rouxel, O.: Reviews and syntheses: The biogeochemical cycle of silicon in the modern ocean, *Biogeosciences*, 18, 1269–1289, <https://doi.org/10.5194/bg-18-1269-2021>, 2021.

715 Villa, G., Fioroni, C., Persico, D., Roberts, A. P., and Florindo, F.: Middle Eocene to Late Oligocene Antarctic glaciation/deglaciation and Southern Ocean productivity, *Paleoceanography*, 29, 223–237, <https://doi.org/10.1002/2013PA002518>, 2014.

720 Virtanen, P., Gommers, R., Oliphant, T. E., Haberland, M., Reddy, T., Cournapeau, D., Burovski, E., Peterson, P., Weckesser, W., Bright, J., Van Der Walt, S. J., Brett, M., Wilson, J., Millman, K. J., Mayorov, N., Nelson, A. R. J., Jones, E., Kern, R., Larson, E., Carey, C. J., Polat, İ., Feng, Y., Moore, E. W., VanderPlas, J., Laxalde, D., Perktold, J., Cimrman, R., Henriksen, I., Quintero, E. A., Harris, C. R., Archibald, A. M., Ribeiro, A. H., Pedregosa, F., Van Mulbregt, P., SciPy 1.0 Contributors, Vijaykumar, A., Bardelli, A. P., Rothberg, A., Hilboll, A., Kloeckner, A., Scopatz, A., Lee, A., Rokem, A., Woods, C. N., Fulton, C., Masson, C., Häggström, C., Fitzgerald, C., Nicholson, D. A., Hagen, D. R., Pasechnik, D. V., Olivetti, E., Martin, E., Wieser, E., Silva, F., Lenders, F., Wilhelm, F., Young, G., Price, G. A., Ingold, G.-L., Allen, G. E., 725 Lee, G. R., Audren, H., Probst, I., Dietrich, J. P., Silterra, J., Webber, J. T., Slavič, J., Nothman, J., Buchner, J., Kulick, J., Schönberger, J. L., De Miranda Cardoso, J. V., Reimer, J., Harrington, J., Rodríguez, J. L. C., Nunez-Iglesias, J., Kuczynski, J., Tritz, K., Thoma, M., Newville, M., Kümmerer, M., Bolingbroke, M., Tartre, M., Pak, M., Smith, N. J., Nowaczyk, N., Shebanov, N., Pavlyk, O., Brodtkorb, P. A., Lee, P., McGibbon, R. T., Feldbauer, R., Lewis, S., Tygier, S., Sievert, S., Vigna, S., Peterson, S., More, S., et al.: SciPy 1.0: fundamental algorithms for scientific computing in Python, *Nat Methods*, 730 17, 261–272, <https://doi.org/10.1038/s41592-019-0686-2>, 2020.



Wagner, T.: Late Cretaceous to early Quaternary organic sedimentation in the eastern Equatorial Atlantic, *Palaeogeography, Palaeoclimatology, Palaeoecology*, 179, 113–147, [https://doi.org/10.1016/S0031-0182\(01\)00415-1](https://doi.org/10.1016/S0031-0182(01)00415-1), 2002.

735 Westacott, S., Planavsky, N. J., Zhao, M.-Y., and Hull, P. M.: Revisiting the sedimentary record of the rise of diatoms, *PNAS*, 118, e2103517118, <https://doi.org/10.1073/pnas.2103517118>, 2021.

Westerhold, T., Marwan, N., Drury, A. J., Liebrand, D., Agnini, C., Anagnostou, E., Barnet, J. S. K., Bohaty, S. M., De Vleeschouwer, D., Florindo, F., Frederichs, T., Hodell, D. A., Holbourn, A. E., Kroon, D., Lauretano, V., Littler, K.,  
740 Lourens, L. J., Lyle, M., Pälike, H., Röhl, U., Tian, J., Wilkens, R. H., Wilson, P. A., and Zachos, J. C.: An astronomically dated record of Earth's climate and its predictability over the last 66 million years, *Science*, 369, 1383–1387, <https://doi.org/10.1126/science.aba6853>, 2020.

Witkowski, J., Harwood, D. M., Wade, B. S., and Brylka, K.: Rethinking the chronology of early Paleogene sediments in the  
745 western North Atlantic using diatom biostratigraphy, *Marine Geology*, 424, 106168, <https://doi.org/10.1016/j.margeo.2020.106168>, 2020.

Witkowski, J., Brylka, K., Bohaty, S. M., Mydlowska, E., Penman, D. E., and Wade, B. S.: North Atlantic marine biogenic  
750 silica accumulation through the early to middle Paleogene: implications for ocean circulation and silicate weathering feedback, *Clim. Past*, 17, 1937–1954, <https://doi.org/10.5194/cp-17-1937-2021>, 2021.

Yool, A. and Tyrrell, T.: Role of diatoms in regulating the ocean's silicon cycle, *Global Biogeochemical Cycles*, 17, 2002GB002018, <https://doi.org/10.1029/2002GB002018>, 2003.

755 Zachos, J., Pagani, M., Sloan, L., Thomas, E., and Billups, K.: Trends, Rhythms, and Aberrations in Global Climate 65 Ma to Present, *Science*, 292, 686–693, <https://doi.org/10.1126/science.1059412>, 2001.

Zhang, Y. G., Pagani, M., Liu, Z., Bohaty, S. M., and DeConto, R.: A 40-million-year history of atmospheric CO<sub>2</sub>, *Phil. Trans. R. Soc. A.*, 371, 20130096, <https://doi.org/10.1098/rsta.2013.0096>, 2013.